

See discussions, stats, and author profiles for this publication at: <https://www.researchgate.net/publication/231647502>

Influence of the Sequence of the Reagents Addition in the Citrate-Mediated Synthesis of Gold Nanoparticles

ARTICLE in THE JOURNAL OF PHYSICAL CHEMISTRY C · JULY 2011

Impact Factor: 4.77 · DOI: 10.1021/jp2017242

CITATIONS

41

READS

31

3 AUTHORS:



Isaac Ojea Jimenez

European Commission

38 PUBLICATIONS 563 CITATIONS

SEE PROFILE



Neus G Bastús

Catalan Institute of Nanoscience and Nanot...

36 PUBLICATIONS 1,236 CITATIONS

SEE PROFILE



Victor Puentes

Catalan Institute of Nanoscience and Nanot...

129 PUBLICATIONS 7,097 CITATIONS

SEE PROFILE

Influence of the Sequence of the Reagents Addition in the Citrate-Mediated Synthesis of Gold Nanoparticles

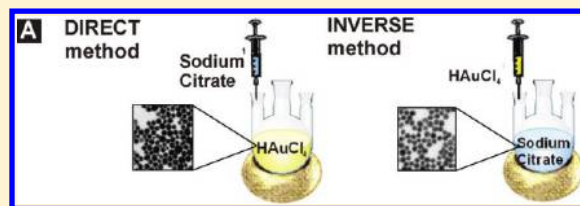
Isaac Ojea-Jiménez,^{*,†} Neus G. Bastús,[†] and Victor Puntes^{*,†,‡}

[†]Institut Català de Nanotecnologia (ICN), Campus UAB, 08193, Cerdanyola del Vallés, Spain

[‡]Institut Català de Recerca i Estudis Avançats (ICREA), 08093, Barcelona, Spain

S Supporting Information

ABSTRACT: The role of sodium citrate (SC) in the formation and growing mechanism of gold nanoparticles was systematically examined. Obtained results show that oxidation of SC can be induced either by the presence of HAuCl₄ or by its thermal decomposition under air. By exchanging the order of reagent addition, it is possible to increase the oxidation rate of SC and hence control the size and morphology, thus allowing preparation of nanoparticles with a narrower size distribution than the standard Turkevich approach.



INTRODUCTION

Gold nanoparticles (Au NPs) and their conjugates have been extensively used in a wide variety of fundamental research and technical applications which include nanobiotechnology, catalysis, and materials science.^{1–3} Since their optical, electric, and catalytic properties are both size- and shape-dependent,^{2,4} great efforts have been dedicated to control the Au NPs mean size, shape, and surface state while routinely producing narrow size distributions.^{2,5–8} Among them, the synthesis of Au NPs based in a single-phase water reduction of tetrachloroauric acid (HAuCl₄) with SC, reported by Turkevich et al. in 1951,⁹ is probably one of the most studied strategies despite its experimental protocol (rapid addition of SC into a hot aqueous solution of HAuCl₄) being little changed over the last 6 decades.^{6,10–12} Especially important is the multiple role played by the SC which acts as (i) reducing agent (driving the reduction of Au³⁺ to Au⁰),^{9,12–16} (ii) capping agent (electrostatically stabilizing the Au NP colloidal solution),^{14,17,18} and (iii) pH mediator (modifying the reactivity of Au species involved in the reaction).^{6,19}

Despite this method allowing control of the Au NPs size from 8 to 150 nm by simply changing the relative concentrations of SC and HAuCl₄,¹¹ the quality (size, size distribution, and morphology)¹² of the obtained NPs is significantly lower than that resulting from nonaqueous solutions.^{20,21} This problem has been traditionally difficult to overcome since a coherent explanation for kinetics of the precursor reduction and particle growth is far more complicated than what its simple experimental protocol suggests.^{6,12,14,22} Therefore, the induction period in the formation of Au NPs seems to be associated with the production of a sufficient number of dicarboxyacetone (DCA) molecules, which were considered to be the active agent that formed gold atoms for the nucleating process.¹⁶ DCA possibly forms a multidentate complex with Au⁺ ions (DCA–Au⁺) and favors the formation of monodisperse spherical particles (Scheme S1, Supporting Information).^{6,14,19,23} This intermediate plays an important role in the disproportionation of aurous species,²⁴ and the formation of small

clusters which grow by the incorporation of new Au⁰ atoms, catalyzed by the nuclei when they are formed.¹⁵ The formation of a DCA intermediate as the oxidation/decarboxylation product from SC has since long been accepted for colloidal Au and Ag NP preparation.^{9,15,19,25}

These facts moved us to systematically examine the role of SC as DCA precursor and the influence of the latter in the growth of Au NPs. Considering that the oxidation of SC can be induced either by the presence of HAuCl₄ or by its thermal decomposition,²⁶ we also decided to change the classical order of reagent addition (injection of HAuCl₄ into a boiling SC solution) in order to increase the conversion ratio of SC to DCA and hence increase the size control in the most employed aqueous Au NPs synthesis. Significantly, the method here presented allows reproducible preparation of Au NPs with an improved size distribution and a uniform spherical shape by simply altering the sequence of reagents addition.

EXPERIMENTAL SECTION

Reagents and Methods. Sodium citrate, 1,3-acetonedicarboxylic acid, and HAuCl₄·3H₂O were purchased from Sigma-Aldrich and stored under Ar atmosphere without further purification steps. Milli-Q water was used in all the experiments unless otherwise stated. Digital images were analyzed with the ImageJ software, and a custom macro performing smoothing (3 × 3 or 5 × 5 median filter), manual global threshold, and automatic particle analysis was provided by the ImageJ. The macro can be downloaded from <http://code.google.com/p/psa-macro>. The particle size was calculated as circle-equivalent diameter from the area of each individual particle ($d = 2(A/\pi)^{1/2}$) and calculating the number averages from the entire

Received: February 21, 2011

Revised: June 27, 2011

Published: July 06, 2011

population or individual peaks found in the histograms. UV–vis absorption spectra were recorded with a Shimadzu UV-2401PC spectrophotometer at room temperature. Au NPs were visualized using transmission electron microscopy (TEM) (JEOL 1010, Japan) at an accelerating voltage of 80 kV. The sample (10 μ L) was drop-cast onto ultrathin Formvar-coated 200-mesh copper grids (Tedpella, Inc.) and allowed to dry in air. For each sample, the sizes of at least 100 particles were measured to obtain the average and the size distribution. Samples were stored in the fridge (+4 $^{\circ}$ C) and were stable for long periods of time (more than 1 year). Each experiment was performed in triplicate. Variations of the calculated mean sizes and size distributions depending of the region of the TEM grid selected for image analysis were not higher than 10% in any case.

Inverting the Order of Reagents Addition. In a typical experiment, an aqueous solution of $\text{HAuCl}_4 \cdot 3\text{H}_2\text{O}$ (0.165 or 0.25 mM) in H_2O (149 mL) was heated up to 100 $^{\circ}$ C for 15 min. The reducing reagent, SC (either 0.34 or 0.26 mmol, respectively) in H_2O (1 mL) was then added (direct method). The same experiment was repeated by maintaining the amounts of reagents but changing the order of reagents addition: an aqueous solution of SC (149 mL) was heated to reflux during 15 min before $\text{HAuCl}_4 \cdot 3\text{H}_2\text{O}$ was added (1 mL) (inverse method). All reactions were maintained at the boiling point for 5 min before cooling them down to room temperature.

Addition of Reducing Agent to Gold Precursor (Direct Method). In a typical experiment, a solution of $\text{HAuCl}_4 \cdot 3\text{H}_2\text{O}$ (1 mL, 25 mM) in H_2O was dissolved in H_2O (149 mL) in a three-neck round-bottom flask and heated up to 100 $^{\circ}$ C for 15 min. The corresponding ratio of reducing reagents (0.34 mmol) (SC: DCA from 100:0 to 0:100) in H_2O (1 mL) was added and the reaction mixture was maintained at boiling temperature for further time before an aliquot was taken and the reaction quenched by cooling the sample in ice–water.

Experiments with pH Variation. In a typical experiment, a solution of $\text{HAuCl}_4 \cdot 3\text{H}_2\text{O}$ (1 mL, 25 mM) in H_2O was dissolved in H_2O (149 mL) in a three-neck round-bottom flask. The pH value of the solution was either left unmodified or increased upon the addition of an aqueous solution of NaOH (150 μ L, 2 M) before heating up to 100 $^{\circ}$ C during 15 min. The reducing reagents SC (0.1 g, 0.34 mmol) and DCA (0.025 g, 0.17 mmol) in H_2O (1 mL) were added and the reaction mixture was maintained at boiling temperature for further time before an aliquot was taken and the reaction quenched by cooling the sample in ice–water.

RESULTS AND DISCUSSION

Inversion of the Order of Reagents Addition. Assuming that the thermal decomposition of a SC solution can lead to the formation of either DCA, acetoacetate, or acetone (Figure S1, Supporting Information),^{14,27,28} and this may improve the final Au NP morphology, we decided to change the traditional order of reagents addition (rapid addition of SC into a hot aqueous solution of HAuCl_4) by heating the SC solution before the addition of the Au^{3+} precursor. For this purpose, we synthesized two different particle batches in which we kept constant the SC:Au ratio (13.6), the temperature (100 $^{\circ}$ C), the final volume (150 mL), and the total reaction time (5 min), while changing the order of reagent addition. These two different procedures were called (i) direct synthesis (addition of sodium citrate into a hot aqueous solution of HAuCl_4) (Figure 1A-left) and (ii) inverse synthesis (addition of an aqueous solution of HAuCl_4 into a boiling sodium citrate solution) (Figure 1A-right). Figure 1B shows the UV–vis spectra of final Au

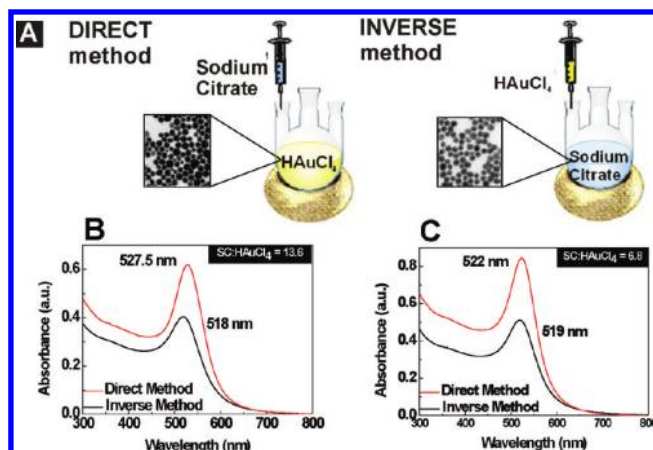


Figure 1. Direct vs inverse sequence of reagents addition (A) and optical (UV–vis spectroscopy) characterization of Au NPs synthesized at 100 $^{\circ}$ C during 5 min under conditions of: (B) 0.165 mM of HAuCl_4 and a SC: HAuCl_4 ratio of 13.6 and (C) under Turkevich conditions (0.25 mM of HAuCl_4 and a SC: HAuCl_4 ratio of 6.8).

NPs synthesized following the above detailed conditions. Surprisingly, the effect of exchanging the order of reagent addition resulted in a dramatic blue shift of the SPR peak from 527.5 nm (direct synthesis) to 518 nm (inverse synthesis) together with a decrease of the maximum absorbance value. Considering that the SPR absorption peak is indicative of particle size,²⁹ this result indicates that Au NPs synthesized by the inverse method are smaller than those synthesized by the direct one. TEM and image analysis (Figure 2) clearly confirmed a decrease of the mean particle size as well as an improvement of Au NP size distribution from 36.6 ± 6.8 nm (SD $\sim 18\%$) (direct synthesis) to 9.0 ± 1.2 nm (SD $\sim 13\%$) (inverse synthesis).

The influence of exchanging the order of reagents was also explored for a relatively lower SC: HAuCl_4 ratio (6.8), by increasing the HAuCl_4 concentration to 0.25 mM while keeping constant the amount of SC added. Consistently with previous experiments, UV–vis spectra depicted in Figure 1C shows again a pronounced blue shift of SPR peak from 522 nm (direct method) to 519 nm (inverse method) accompanied by a decrease of the absorbance maximum. Particle morphology analyzed by TEM (Figure 2) reveals a decrease of both Au NP mean size and polydispersity from 17.8 ± 2.5 nm (SD $\sim 14\%$) (direct synthesis) to 14.9 ± 1.5 nm (SD $\sim 10\%$) (inverse synthesis). In all cases, kinetics of Au NP formation correlated with the changes of the color of the solution. Thus, using a SC:Au ratio of 13.6, the inverse order reaction needed 4 min to turn from purple to red, while in the case of the direct method changes in color were reached after approximately 8 min. Similar results were found in the case of Au NP synthesis using a 6.8 SC:Au ratio. Changes in the color of Au NPs solution have been correlated with the consumption of AuCl_4^- ions, the oxidation of SC, and the subsequent formation of DCA.¹⁰ Considering that a short induction time (faster Au NP formation) can be correlated with a very fast DCA formation, our results suggest that by heating SC before the addition of Au^{3+} precursor it is possible to induce the oxidation of a fraction of SC. Similar results were found by Xia et al.,¹⁹ who demonstrated that the oxidation of SC to DCA can be increased by using Ag^+ ions, obtaining Au NPs with a higher quality in terms of size and shape distributions.

Presence of DCA in the Reducing Mixture. In order to study how the DCA influences the final size and size distribution of Au NPs, we performed a set of experiments by changing the molar

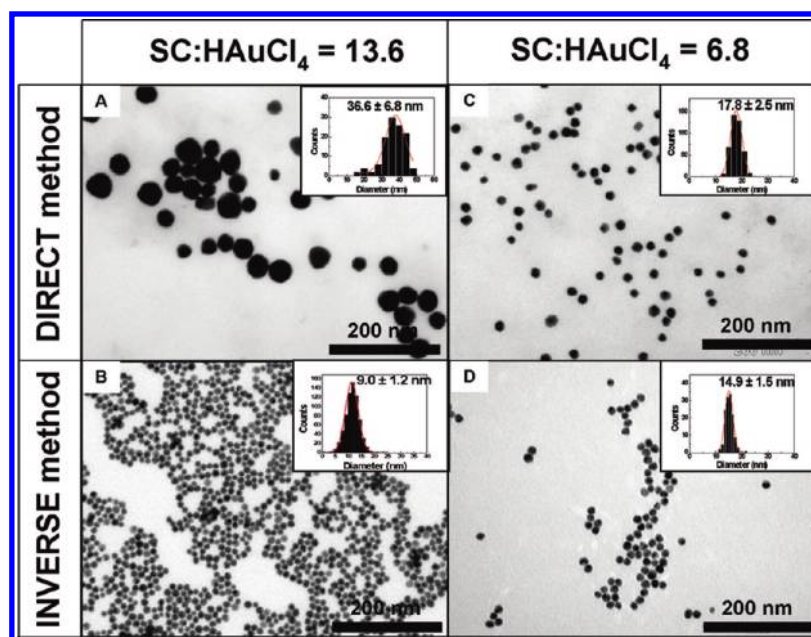


Figure 2. Morphological (TEM) characterization of Au NPs synthesized at 100 °C during 5 min (A, B) under conditions of 0.165 mM of HAuCl_4 and a SC: HAuCl_4 ratio of 13.6 and (C, D) under Turkevich conditions (0.25 mM of HAuCl_4 and a SC: HAuCl_4 ratio of 6.8); under both direct and reverse sequence of reagent addition in each case. Inset graphs in TEM images show size distribution measurements of Au NPs.

mass fraction of DCA in a reducer mixture composed by SC and DCA. Note that SC was always in large excess (approximately 93%, see Supporting Information) and also that previous studies revealed its role as a reducing reagent is not the size controlling factor.⁶ In detail, an aqueous gold precursor solution of HAuCl_4 0.165 mM was heated to boil and the reducer mixture (SC + DCA) was added (direct synthesis). The reducer mixture to HAuCl_4 ratio was kept constant (13.6), and the SC:DCA ratios used in the reducer mixture were systematically varied from 100:0 to 50:50. In all cases, kinetics of particle formation assessed by time evolution UV–vis spectroscopy show that the progressive substitution of SC by DCA leads to higher reaction rates (faster Au NPs formation). Thus, with a SC:DCA ratio of 100:0 (no DCA present in the reducer mixture, Figure 3A) the reaction needs 11 min to reach its final stage (i.e., when no further evolution was observed), while this time decreases down to 5 min (Figure 3B) or 4 min (Figure 3C) when the amount of DCA increased to SC:DCA (90:10) and (50:50), respectively. Interestingly, the SPR peak initially blue shifts from 523 to 519 nm when increasing the molar amount of DCA from 100:0 to 90:10 (SC:DCA) of the reducing mixture, respectively, but quite unexpectedly goes back to 523 nm when using a 50:50 ratio of reducers. Considering that the position of the SPR band is closely associated to the mean size of Au NPs solution,³⁰ these results indicate that (i) the kinetic of Au NP formation (reaction rate) depends on the amount of SC and DCA present in solution and (ii) it drastically influences the Au NPs morphology (size and shape). This effect will become more apparent after we examine the resulting pH from the different reaction mixtures later in this article (vide infra). Further TEM analysis, performed when the Au NPs showed no further evolution by UV–vis, confirmed that the final size and morphology depend on the SC:DCA ratio employed. Thus, the presence of 10% of DCA in the reducing mixture yields lower sizes but larger concentrations of Au NPs (17.7 ± 2.0 nm, SD $\sim 11\%$) in comparison with the 100:0

(SC:DCA) (21.2 ± 3.2 nm, SD $\sim 15\%$) (Figure 3D,E), which is in agreement with the faster reaction rate observed by UV–vis spectroscopy. By contrast, the monodispersity was drastically spoiled in the case of a 50:50 (SC:DCA) ratio (25.9 ± 5.8 nm, SD $\sim 22\%$) (Figure 3F), which would explain the SPR peak appearing at 523 nm. Surprisingly, when the SC:DCA ratio used was 0:100, no particle formation was detected by UV–vis spectroscopy after more than 3 h of reaction, opposite to what was previously reported.¹⁶ This observation made us to consider which form of DCA was actually employed by Turkevich and co-workers. In our case, the resulting solution had a pH value of 3.7, which could explain the poor observed reactivity due to protonation of the carboxylic functionalities of DCA, thus making them less prone to oxidation/decarboxylation. This result indicates that although both a decrease in the pH and an increase in DCA accelerate the reduction process leading to an improvement of the final Au NPs size distribution, DCA is not able to reduce the Au^{3+} ions by itself at acidic pH.

Effect of the pH. The discovery of Peng and co-workers that the pH-dependent reactivity of the Au^{3+} precursor plays a determining role in this system was tested by controlling the pH value of the reaction solution.⁶ Since the final pH of the mixture should depend on the relative concentration of SC, DCA, and HAuCl_4 , the pH values of the reaction solutions were measured at room temperature with the designated solution compositions, that is, changing the relative molar mass fraction of SC:DCA (100:0, 90:10, and 50:50) in a solution of 0.165 mM HAuCl_4 . A subtle pH variation from pH 6.2 to 5.9 was observed upon decreasing the amount of the weak base, SC, present in the reducing mixture from a ratio of 100:0 to 90:10, respectively. It is known that the particle size can be tuned by changing the pH, which affects the reactivity of gold complexes reflected by their reduction potential.³¹ In the range of pH = 3.3–6.2 only the very reactive $\text{AuCl}_3(\text{OH})^-$ ion exists in the reaction solution. According to the results of Peng et al.,⁶ both reactions are in the low pH

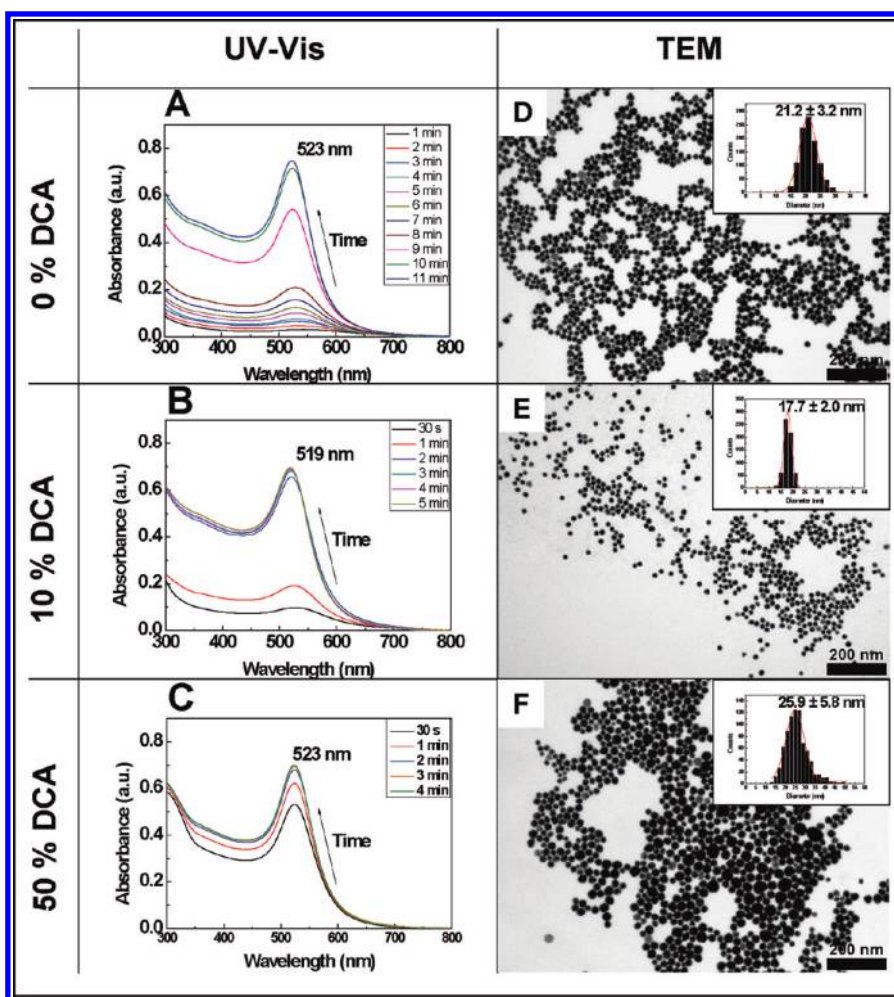


Figure 3. Optical (UV-vis spectroscopy) and morphological (TEM) characterization of Au NPs synthesized at 0.165 mM of HAuCl₄ and a SC:HAuCl₄ ratio of 13.6 at 100 °C, under different ratios of the reducing mixture SC:DCA: 100:0 (A, D); 90:10 (B, E), and 50:50 (C, F). Inset graphs in TEM images show size distribution measurements of Au NPs.

evolution regime which consists of three overlapping steps: nucleation, random attachment to polycrystalline nanowires, and intraparticle ripening. However, the differences observed in the SPR peak, Au NPs size, and reaction rate were significant enough to make us envisage a different factor, apart from the pH value, responsible for the observed trends. By contrast, the pH of the reaction solution with a 50:50 ratio of SC:DCA was found to be 4.1, which in this case can be considered responsible of the increased reaction rate and the observed size/shape evolution.⁶

To determine which of the two factors (i.e., amount of DCA vs pH of the reaction solution) had a more significant effect in the synthesis of Au NPs, we carried out a simple key experiment. The pH influence on the size/shape evolution was studied for two reactions with different pH values but both at fixed SC:HAuCl₄ and DCA:HAuCl₄ ratios of 13.6 and 6.8 respectively, and initial Au³⁺ concentration of 0.165 mM. One of the reactions was left at the resulting pH value of 5.1, while the other was adjusted to pH 6.2 (by adding 0.1 M NaOH) in order to compare with the experiment of panels A and D of Figure 3 (vide infra). From the kinetics of particle formation by UV-vis spectroscopy, both reactions took place in a similar time scale than the previous reaction of Figure 3C with the

same DCA:HAuCl₄ ratio (6.8), thus reaching its final stage in less than 4 min (Figure 4A,B). It is also interesting to compare the corresponding SPR peaks of the final products between all three reactions (Figures 3C, 4A, and 4B), which blue shifted from 523 to 521 and 517 nm upon increasing the pH value of the solution (from pH 4.1 to 5.1 and 6.2, respectively). TEM analysis confirmed a decrease of the size and an improvement of the monodispersity (from 15.7 ± 3.6 nm (SD ~ 23%) to 14.6 ± 2.0 nm (~13%)) when the pH value was adjusted from 5.1 to 6.2 for the reactions of panels C and D of Figure 4, respectively. Finally, these experiments are clear evidence that the presence of DCA in the reaction mixture induced both a decrease of the NP size and an improvement of the monodispersity when the pH of the solution was not drastically changed (for a pH value of 6.2). This was confirmed by comparing both the peak shift in UV-vis (from 523 to 517 nm) between Figures 3A and 4B, respectively, and TEM analysis (from 21.2 ± 3.2 nm (~15%) to 14.6 ± 2.0 nm (~13%)) between Figures 3D and 4D, respectively. Finally, the effect of DCA on the Au NP synthesis also implied an increase on the reaction rate, which could not be attributed to a pH variation in this case. This specific example strongly suggests that the presence of DCA induces the rapid formation of DCA-Au⁺

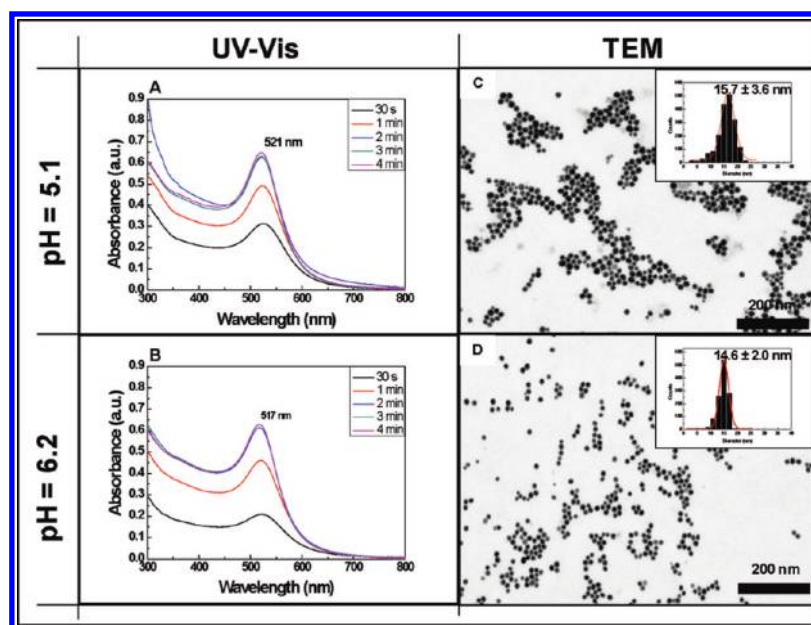


Figure 4. Optical (UV–vis spectroscopy) and morphological (TEM) characterization of Au NPs synthesized at 100 °C, 0.165 mM HAuCl₄, and SC: HAuCl₄ and DCA:HAuCl₄ ratios of 13.6 and 6.8, respectively. The pH of the reactions was either left unmodified at 5.1 (A, C) or adjusted to pH = 6.2 (B, D). Inset graphs in TEM images show size distribution measurements of Au NPs.

complexes, thus favoring the formation of precursor stable particles and leading to narrower size distribution.

CONCLUSIONS

In summary, we have developed a simple strategy to synthesize monodisperse spherical Au NPs in aqueous solution via citrate reduction of HAuCl₄. As compared with the commonly used Turkevich method, the main distinct feature of our approach is the injection of the HAuCl₄ precursor into a hot SC solution. Because of this new modification, the oxidation of the SC partially takes place before the addition of the HAuCl₄ solution leading to a significant increase of the nucleation and growth rate, which largely narrow the Au NP size distribution. The change in the sequence of reagents addition substantially reduces the inhomogeneous mixing of the citrate solution with the HAuCl₄ solution, which is responsible for the inhomogeneous nucleation and thus for the temporal overlap between nucleation and crystal growth (i.e., broad size distribution).¹⁹ All in all, the obtained results also experimentally demonstrate the importance of DCA intermediate on the final NP morphology and shed light into the mechanism of reduction of Au³⁺ species in the most commonly employed recipe for Au NPs preparation in water.

ASSOCIATED CONTENT

S Supporting Information. Reaction scheme of all species involved in the formation of Au NPs, HPLC analysis showing both the formation of DCA as well as decomposition of SC, and time evolution of the UV–vis absorbance spectra of Au NPs at 90 °C. This material is available free of charge via the Internet at <http://pubs.acs.org>.

AUTHOR INFORMATION

Corresponding Author

*E-mail: isaac.ojea.icn@uab.es, victor.puntes@uab.es. Homepage: <http://www.nanocat.org/>.

ACKNOWLEDGMENT

We thank Mr. Manuel Plaza from Departament d'Enginyeria Química of UAB for HPLC analyses and Dr. Josep Maria Campanera from Department of Pharmaceutical Sciences of UB for fruitful discussions.

REFERENCES

- (1) Bastús, N. G.; Sánchez-Tilló, E.; Pujals, S.; Farrera, C.; López, C.; Giral, E.; Celada, A.; Lloberas, J.; Puntes, V. F. *ACS Nano* **2009**, *3*, 1335–1344.
- (2) Daniel, M. C.; Astruc, D. *Chem. Rev.* **2004**, *104*, 293–346.
- (3) Kogan, M. J.; Bastús, N. G.; Amigo, R.; Grillo-Bosch, D.; Araya, E.; Turiel, A.; Labarta, A.; Giral, E.; Puntes, V. F. *Nano Lett.* **2006**, *6*, 110–115.
- (4) Burda, C.; Chen, X.; Narayanan, R.; El-Sayed, M. A. *Chem. Rev.* **2005**, *105*, 1025–1102.
- (5) Jana, N. R.; Gearheart, L.; Murphy, C. J. *Langmuir* **2001**, *17*, 6782–6786.
- (6) Ji, X.; Song, X.; Li, J.; Bai, Y.; Yang, W.; Peng, X. *J. Am. Chem. Soc.* **2007**, *129*, 13939–13948.
- (7) Murphy, C. J.; Jana, N. R. *Adv. Mater.* **2002**, *14*, 80–82.
- (8) Nikoobakht, B.; El-Sayed, M. A. *Chem. Mater.* **2003**, *15*, 1957–1962.
- (9) Turkevich, J.; Stevenson, P. C.; Hillier, J. *Discuss. Faraday Soc.* **1951**, *11*, 55–75.
- (10) Chow, M. K.; Zukoski, C. F. *J. Colloid Interface Sci.* **1994**, *165*, 97–109.
- (11) Frens, G. *Nature (London), Phys. Sci.* **1973**, *241*, 20–22.
- (12) Kimling, J.; Maier, M.; Okenve, B.; Kotaidis, V.; Ballot, H.; Plech, A. *J. Phys. Chem. B* **2006**, *110*, 15700–15707.
- (13) Ojea-Jiménez, I.; Romero, F. M.; Bastús, N. G.; Puntes, V. *J. Phys. Chem. C* **2010**, *114*, 1800–1804.
- (14) Kumar, S.; Gandhi, K. S.; Kumar, R. *Ind. Eng. Chem. Res.* **2007**, *46*, 3128–3136.
- (15) Rodríguez-González, B.; Mulvaney, P.; Liz-Marzán, L. M. *Z. Phys. Chem.* **2007**, *221*, 415.
- (16) Turkevich, J.; Stevenson, P. C.; Hillier, J. *J. Phys. Chem.* **1953**, *57*, 670–673.

- (17) Henglein, A.; Giersig, M. *J. Phys. Chem. B* **1999**, *103*, 9533–9539.
- (18) Ojea-Jimenez, I.; Puentes, V. *J. Am. Chem. Soc.* **2009**, *132*, 5322–5322.
- (19) Xia, H.; Bai, S.; Hartmann, J. R.; Wang, D. *Langmuir* **2009**, *26*, 3585–3589.
- (20) Puentes, V. F.; Krishnan, K. M.; Alivisatos, A. P. *Science* **2001**, *291*, 2115–2117.
- (21) Talapin, D. V.; Rogach, A. L.; Kornowski, A.; Haase, M.; Weller, H. *Nano Lett.* **2001**, *1*, 207–211.
- (22) Pong, B. K.; Elim, H. I.; Chong, J. X.; Ji, W.; Trout, B. L.; Lee, J. Y. *J. Phys. Chem. C* **2007**, *111*, 6281–6287.
- (23) Privman, V.; Goia, D. V.; Park, J.; Matijevic, E. *J. Colloid Interface Sci.* **1999**, *213*, 36–45.
- (24) Gammons, C. H.; Yu, Y.; Williams-Jones, A. E. *Geochim. Cosmochim. Acta* **1997**, *61*, 1971–1983.
- (25) Wu, X.; Redmond, P. L.; Liu, H.; Chen, Y.; Steigerwald, M.; Brus, L. *J. Am. Chem. Soc.* **2008**, *130*, 9500–9506.
- (26) Barbooti, M. M.; Al-Sammerrai, D. A. *Thermochim. Acta* **1989**, *98*, 119–126.
- (27) Munro, C. H.; Smith, W. E.; Garner, M.; Clarkson, J.; White, P. C. *Langmuir* **1995**, *11*, 3712–3720.
- (28) Xue, C.; Metraux, G. S.; Millstone, J. E.; Mirkin, C. A. *J. Am. Chem. Soc.* **2008**, *130*, 8337–8344.
- (29) Link, S.; El-Sayed, M. A. *J. Phys. Chem. B* **1999**, *103*, 8410–8426.
- (30) Hostetler, M. J.; Wingate, J. E.; Zhong, C.-J.; Harris, J. E.; Vachet, R. W.; Clark, M. R.; Londono, J. D.; Green, S. J.; Stokes, J. J.; Wignall, G. D.; Glish, G. L.; Porter, M. D.; Evans, N. D.; Murray, R. W. *Langmuir* **1998**, *14*, 17–30.
- (31) Goia, D. V.; Matijevic, E. *Colloids Surf., A* **1999**, *146*, 139–152.